Organic & Biomolecular Chemistry

Accepted Manuscript

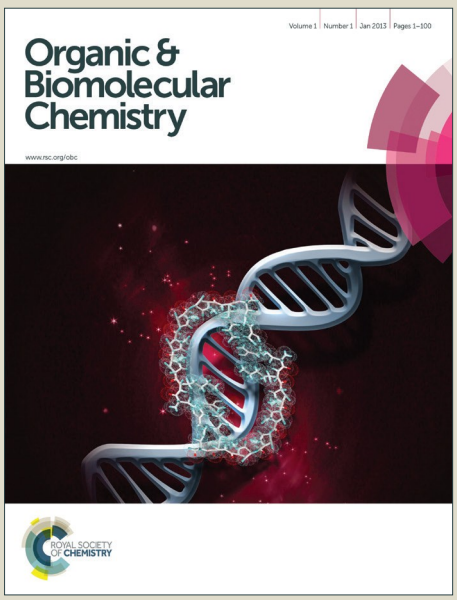

ROYAL SOCIETY OF CHEMISTRY

www.rsc.org/obc

Organic and Biomolecular Chemistry

FULL PAPER

In Silico Screening of Molecular Imprinting Prepolymerization Systems: Oseltamivir Selective Polymers through Full-system Molecular Dynamics-based Studies

Received 00th January 20xx,
Accepted 00th January 20xx

DOI: 10.1039/x0xx00000x

www.rsc.org/

Siamak Shoravi,[a§] Gustaf D. Olsson,[a§] Björn C. G. Karlsson,[a] Fredrik Bexborn,[a] Younes Abghoui, [a†‡] Javed Hussain,[a†‡] Jesper G. Wiklander [a] and Ian A. Nicholls[a,b*]

All-component molecular dynamics studies were used to probe a library of oseltamivir molecularly imprinted polymer prepolymerization mixtures. Polymers included one of five functional monomers (acrylamide, hydroxyethylmethacrylate, methacrylic acid, 2-(triflouromethyl)acrylic acid, 4-vinylpyridine) and one of three porogens (acetonitrile, chloroform, methanol) combined with the crosslinking agent ethylene glycol dimethacrylate and initiator 2,2'-azobis(2-methylpropionitrile). Polymers were characterized by nitrogen gas sorption measurements and SEM, and affinity studies performed using radioligand binding in various media. In agreement with the predictions made from the simulations, polymers prepared in acetonitrile using either methacrylic or trifluoromethacrylic acid demonstrated the highest affinities for oseltamivir. Further, the ensemble of interactions observed in the methanol system provided an explanation for the morphology of polymers prepared in this solvent. The materials developed here offer potential for use in solid-phase extraction or for catalysis. The results illustrate the strength of this *in silico* strategy as a potential prognostic tool in molecularly imprinted polymer design.

Introduction

The diversity of structures that can be recognized by antibodies and the impressive selectivities that they often demonstrate have made them an important tool in biomedicine and analytical science.[1] Efforts to develop biomimetic materials with antibody-like recognition characteristics have been driven by several factors including; fundamental interest in biomolecular recognition, the needs of analytical science, and the desire to establish novel therapies and medical devices.[2] Molecular imprinting is one of the most promising methods for the preparation of biomimetic materials and can be used to produce highly selective synthetic receptors for molecular structures spanning from ions to biomacromolecules.[3–9] The method involves the formation of cavities in a synthetic polymer matrix that are of complementary functional and structural character to a template molecule/entity. The ability of a molecularly imprinted polymer (MIP) to selectively recognize and bind the template structure in the presence of closely related chemical species has made them of interest for use in a range of biomedical and biotechnological applications.[10–13] Furthermore, although molecular imprinting carries parallels to the immune system's production of antibodies, it also offers significant contrasts and even advantages, such as thermal and chemical stability,[14] relatively low cost of production, and no requirement for hapten conjugation protocols.

The interest in molecular imprinting has driven the development of a number of experimental[15–17] and theoretical strategies[18–20] for studying MIP systems and for designing or selecting polymers. Over more recent years the power of all-component (full system) molecular dynamics (MD) studies of MIP prepolymerization systems[21] as a diagnostic tool for aiding in the elucidation of mechanisms underlying polymer performance, or lack thereof, has been demonstrated through an increasing number of studies.[22–28] The molecular-level understanding obtained using this approach raised the possibility for employing such full-system MD-strategies in a prognostic capacity, namely for the in silico screening of polymer libraries. Accordingly, we elected to investigate the use of this MD-approach for the screening of candidate molecularly imprinted polymers, here using the antiviral substance oseltamivir, the active constituent in the anti-

[a] Bioorganic & Biophysical Chemistry Laboratory, Linnaeus University Centre for Biomaterials Chemistry, Department of Chemistry & Biomedical Sciences, Linnaeus University, SE-391 82 Kalmar, Sweden. * Email: ian.nicholls@lnu.se
[b] Department of Chemistry - BMC, Uppsala University, Box 576, SE-751 23, Uppsala, Sweden.
§ These authors contributed equally
† These authors contributed equally
‡ Present address: Science Institute, Faculty of Physical Sciences, University of Iceland
Electronic Supplementary Information (ESI) available: Materials characterization - elemental analysis, FT-IR spectra, SEM, nitrogen sorption (BET), porosity (BJH) and laser diffraction studies. See DOI: 10.1039/x0xx00000x

influenza drug Tamiflu®, as template. Yang *et al.*[29] have reported a study on the impact of two functional monomers (acrylamide and 4-VP) on oseltamivir imprinted polymer recognition in the establishment of an LC-MS-based assay. Although the mechanisms of template-recognition in these polymers wasn't apparent, the differences in performance suggest the use of more detailed studies.

Our choice of this template was motivated by the need for materials capable of selectively recognizing oseltamivir. This need is derived from the significant risks to society posed by the potential spread of new strains of influenza with human pathogenicity or with impact on agriculture. Our capacity to challenge the threat of the virus is dependent upon our ability to develop new vaccines, and upon our access to effective virus-targeted small molecule pharmaceuticals. The small molecule weapons targeting the influenza virus capsid protein neuraminidase, namely oseltamivir (Tamiflu)[30–32] (Chart 1) and zanamivir (Relenza),[33] currently form our last line of defence against this virus. More recently, the identification of strains resistant to this class of substances has roused serious concern.[34–36] Equally as worrying is the clear evidence of the presence of these substances in the world's water systems, a factor that can contribute to resistance development.[37] Accordingly, the development of methods for the rapid and sensitive determination of these substances in the environment is required. Furthermore, monitoring necessitates that sensors are robust and are able to withstand the rigors (e.g. extremes of temperature, exposure to complex matrices) of environments not normally conducive to biomacromolecular stability.

In the present study, we have explored the potential of full-system MD-based techniques as a prognostic tool through the screening of a library of prepolymerization mixtures in order to identify polymerization systems capable of affording MIPs with selectivity for oseltamivir. Such materials offer scope for use in a variety of applications, which shall be reported in due course. Importantly, the in silico screening identified polymerization systems leading to MIPs with selectivities for the template that were not readily identifiable by pure intuition. Furthermore, the MD-studies provided valuable insights into the mechanisms underlying template recognition in these molecularly imprinted materials.

Experimental

Theoretical studies

MD simulations of prepolymerization mixtures were conducted using an approach initially developed by Karlsson *et al.*[21] and further refined by Olsson *et al.*[23] based upon the AMBER (v. 10, UCSF San Francisco, CA) suite of programs.[38–40] Briefly, MIP prepolymerization mixtures were initially built using PACKMOL,[41,42] utilizing a protocol based on a template – functional monomer – crosslinking monomer stoichiometry of 1:12:55 (see Chart 1 and Table 1 for the nature and number of components in each simulated prepolymerization mixture). All systems were parameterized using a combination of the Amber force field FF03[43] and the general amber force field (GAFF),[44] assigning partial atomic charges using the AM1-BCC method implemented in the ANTECHAMBER module. Mixtures were then energy minimized, to avoid high-energy vdW contacts between each of the packed components, using a combination of the steepest descent and conjugate gradient algorithms (in total 10^3 steps). Mixtures were subsequently heated from 0 K to 293 K at conditions of constant volume, NVT, (300 ps, employing the Langevin thermostat and a collisional frequency of 1.0 ps^{-1}) prior to an isothermal equilibration step at NPT (1.1 ns, T=293 K, P=1 bar, isotropically controlled pressure using the Langevin barostat and an pressure relaxation time constant of 2.0 ps) to achieve stable values in energy, pressure and density. Finally, 10 ns of production-phase data was collected for each system under conditions of NVT. During MD simulations, periodic boundary conditions (PBC) were employed in all directions in conjunction with a 9 Å cut-off for non-bonded interactions. Beyond this cut-off, the particle mesh Ewald (PME)[45] method was used to better describe long-range electrostatic interactions whereas vdW interactions were treated through an implemented correction for energy and pressure. The SHAKE algorithm was used to constrain all bonds to hydrogen to permit use of a 0.002 ps time-step. To better describe variation in observed prepolymerization interaction data, each mixture was simulated in quadruplicate after initially building the systems with different starting coordinates (PACKMOL). Production-phase trajectories were analyzed using the PTRAJ module in AMBER to extract the degree of complexation between the components in each of the simulated MIP prepolymerization mixtures. All hydrogen bond interactions formed during MD simulations were extracted from trajectory data using a bond and angle cut-off of 3.0 Å and 60 degrees, respectively.

Chemicals

Acrylamide (ACA), hydroxyethylmethacrylate (HEMA), methacrylic acid (MAA), 2-(trifouromethyl)acrylic acid (TFMAA), 4-vinylpyridine (4VP), ethylene glycol dimethacrylate (EGDMA), chloroform ($CHCl_3$), acetonitrile (ACN), methanol (MeOH), toluene (TOL), chloroform-d ($CDCl_3$) and acetic acid (AcOH) where all purchased from Sigma-Aldrich (Germany). Ethanol (EtOH, 99.5%) was from Solveco (Sweden), 2,2'-azobis(2-methylpropionitrile (AIBN) was purchased from Fluka (Germany). All chemicals and solvents were of analytical grade. [^{3}H]-Oseltamivir (specific activity 15 Ci/mmol) was from American Radiolabeled Chemicals Inc. (St. Louis, MO, USA). Tamiflu (Roche, Switzerland) was obtained as 75 mg oral capsules (see Chart 1 for structures).

MAA, HEMA and 4VP, were purified by vacuum distillation and kept at -20 °C until use. Distilled HEMA was passed through activated Al_2O_3 prior to use. ACA and TFMAA were used as purchased. EGDMA was purified by extraction from a mixture of 75 ml 0.1 M $NaOH_{(aq)}$ and 25 mL brine (three times), washed with 25 mL of saturated $NaCl_{(aq)}$, dried over anhydrous magnesium sulfate and filtered. EGDMA was passed over activated Al_2O_3 prior to use. $CHCl_3$ was washed with dH_2O and

dried over $CaCl_2$ prior to distillation and refluxed with $CaCl_2$ and distilled. ACN was dried over molecular sieves overnight following addition of CaH_2 prior to distillation until no further gas was evolved and distilled. The distilled solvent was stored in a bottle containing molecular sieves. All chemicals were stored in a cold room at 6-8 °C until use.

Extraction of oseltamivir

The template, oseltamivir, the active substance of Tamiflu (Roche), was extracted by mixing the content of 30 capsules in 20 mL distilled H_2O with rigorous vortexing, following by ten minutes of sonication at 30 °C with subsequent centrifugation at 14000 x g for 15 minutes. The supernatant was withdrawn and the sediment was reconstituted in 10 mL of dH_2O followed by further sonication and centrifugation as above. The supernatants were pooled and after a further centrifugation the supernatant was filtered through 45 and 20 μm PVDF syringe filters. The filtered solution was mixed with 20 ml $CHCl_3$ and stirred well during drop wise addition of $NaOH_{(aq)}$ (2 and 0.5 M). The pH of the aqueous solution was inspected continuously using pH-paper and the addition of $NaOH_{(aq)}$ was stopped after a pH of 9-10 was achieved. The $CHCl_3$ was collected and the aqueous phase extracted with chloroform (3 x 10 mL). The organic phases were combined and filtered trough 45 and 20 μm pore filters and washed with 20 mL brine and subsequent 3 x 20 mL dH_2O and dried using calcium chloride following the evaporation of solvent using a rotary evaporator. The resulting off-white solid was dried under vacuum. The identity was confirmed by ^{1}H-NMR spectroscopy (Varian INOVA 500 MHz instrument) using $CDCl_3$ as solvent.[46]

Polymer synthesis and work up

A series of oseltamivir MIPs and their corresponding non-imprinted polymers (REFs) was synthesized based upon copolymers of the functional monomers 4VP, ACA, HEMA, MAA or TFMAA and the crosslinking monomer EGDMA, using $CHCl_3$, ACN or MeOH as porogenic solvent (see Table 1 for compositions of polymer systems). The prepolymerization mixtures were prepared in 50 mL centrifuge glass tubes and mixed thoroughly by vortexing, following by sonication (30 s) in an ultra sound water bath (20 °C). The reference polymer mixtures were prepared similarly, though in the absence of the template. The reaction tubes were placed in a liquid nitrogen bath (15 min) before application of vacuum for 10 min before thawing. The freeze-thaw cycle was repeated three times. The reaction tubes were sealed and exposed to UV-light (100W Sylvania H44GS black ray lamp, 320 nm) for 12 h at 20 °C.

Resultant bulk polymers were ground using a Fritsch Pulverisette 14 with grater shred sizes of 0.5, 0.2 and 0.12 mm before wet sieving with acetone through sieves of the mesh sizes of 63 then 25 μm. The polymer particles within the size range 25-63 μm were subjected to repeated sedimentation from acetone to remove eventual smaller particles. Polymer (4 g) was placed in an HPLC column and washed using mixtures of EtOH-AcOH (500 mL, 4:1 v/v), EtOH (100 mL), methanol-aqueous NaOH (aq, 5 M)-water (200 mL, 5:2:3 v/v/v), MeOH (100 mL), MeOH-AcOH-water (200 mL, 18:1:1 v/v/v), MeOH (300 mL) and finally acetone (100 mL). The washed polymer particles were removed from the column using acetone, then air- and vacuum-dried before being stored in sealed sample tubes until used.

Polymer characterization

Polymer particles were studied by scanning electron microscopy (SEM), elemental analysis (CHN), specific surface area (Brunauer, Emmett, and Teller, BET), porosity (Barrett-Joyner-Halenda, BJH), fourier transform infrared spectroscopy (FT-IR) and size determination. SEM analyses were performed in Linköping University Sweden, on a Leo 1550 Gemini instrument with a field emission electron gun. Alumina stubs attached to a carbon disc and coated with a thin layer of platinum, utilizing a platinum sputtering unit LEICA EM SCD 500, were used to immobilize the polymer particles prior to analysis with the instrument using a 3 kV electron beam. Elemental analyses, CHN, were performed by MikroKemi AB, Uppsala, Sweden. BET[47] nitrogen sorption surface area analysis and BJH[48] porosity measurements were carried out at the Department of Chemical Engineering, Lund University, Lund, Sweden. Samples were dried and degased under vacuum at 50 °C for 16 h. N_2 pressures were determined at 43 measurement points with 20 s of equilibrium time for the adsorption and desorption isotherms, respectively. The pore sizes were calculated at 0.9950 relative pressures. FT-IR spectroscopic studies were performed using a Perkin-Elmer Spectrum 100 FT-IR spectrometer, with a connected Perkin-Elmer FT-IR microscope *i*-series for diffuse reflectance method on powdered samples that were milled together with dry KBr. Samples were scanned 32 times with bidirectional scanning from 4000 cm^{-1} to 450 cm^{-1} with a resolution of 16 cm^{-1}, scanning at constant velocity of 1.5 cm/s and strong apodization of signals detected on a mercury cadmium telluride (MCT) detector. Particle size determinations were performed using a Malvern Mastersizer MS20 instrument (Malvern, UK).

Radio ligand polymer titration

Polymer particles (25-63 μm) were suspended in ACN, TOL and 10 mM phosphate buffer pH 7.0 to a concentration of 10.0 mg polymer/mL. From the stock suspensions, volumes corresponding to final concentrations of 0.1, 0.25, 0.5, 1.0, 2.5 and 5.0 mg polymer/mL and 50.0 μl [3H]-Oseltamivir were added to incubation tubes containing corresponding solutions resulting in a total volume of 1.0 mL. All samples were prepared in triplicate and incubations in ACN and TOL were performed both with and without the addition of AcOH to a final concentration of 0.5% (v/v) in order to minimize nonspecific binding. Samples were incubated on a rocking table for 3 h at 21 °C. The samples were then centrifuged at 20800 rcf for 10 min and a 600 μL aliquot of supernatant was transferred into a scintillation tube (6.0 mL) containing 2.0 mL of scintillation cocktail (Ready safe, Beckman Coulter) following by rigorous vortexing. The radioactivity of the samples was then measured with a Packard TRI-CARB 2100 TR liquid scintillation analyzer.

Table 1 Molecularly imprinted polymer compositions[a]

	Amount (mmol)						
Polymer system	Oseltamivir	Monomer	EGDMA	AIBN	$CHCl_3$	ACN	MeOH
MAA-$CHCl_3$	1.3 [10][b]	15.6 [120]	75.5 [550]	1.2 [10]	237 [2278]		
MAA-ACN	1.3 [10]	15.6 [120]	75.5 [550]	1.2 [10]		237 [3490]	
MAA-MeOH	1.3 [10]	15.6 [120]	75.5 [550]	1.2 [10]			237 [4499]
TFMAA-$CHCl_3$	1.3 [10]	15.6 [120]	75.5 [550]	1.2 [10]	237 [2410]		
TFMAA-ACN	1.3 [10]	15.6 [120]	75.5 [550]	1.2 [10]		237 [3693]	
TFMAA-MeOH	1.3 [10]	15.6 [120]	75.5 [550]	1.2 [10]			237 [4761]
ACA-$CHCl_3$	1.3 [10]	15.6 [120]	75.5 [550]	1.2 [10]	237 [2245]		
ACA-ACN	1.3 [10]	15.6 [120]	75.5 [550]	1.2 [10]		237 [3439]	
ACA-MeOH	1.3 [10]	15.6 [120]	75.5 [550]	1.2 [10]			237 [4434]
HEMA-$CHCl_3$	1.3 [10]	15.6 [120]	75.5 [550]	1.2 [10]	246 [2366]		
HEMA-ACN	1.3 [10]	15.6 [120]	75.5 [550]	1.2 [10]		246 [3625]	
HEMA-MeOH	1.3 [10]	15.6 [120]	75.5 [550]	1.2 [10]			237 [4763]
4VP-$CHCl_3$	1.3 [10]	15.6 [120]	75.5 [550]	1.2 [10]	23.7 [2333]		
4VP-ACN	1.3 [10]	15.6 [120]	75.5 [550]	1.2 [10]		237 [3574]	
4VP-MeOH	1.3 [10]	15.6 [120]	75.5 [550]	1.2 [10]			237 [4609]

[a] Reference polymers were prepared with similar composition though in the absence of the template, oseltamivir. [b] Figures in parentheses are the number of molecules included in the molecular dynamics simulations of the corresponding prepolymerization mixture.

Competitive experiments

The competitive binding studies were performed in triplicate essentially as described above using ACN and TOL containing 0.5% AcOH (v/v) as well as 10 mM phosphate buffer pH 7.0. Polymer samples (0.75 mg from a stock slurry) were incubated together with 50 µl [^{3}H]-oseltamivir and 5.0 µl unlabeled oseltamivir with final concentrations of 10 nM to 10 mM. The samples were then treated as described previously and the radioactivity of unbound ligand in the 600 µL aliquot of supernatant from centrifuged samples was determined as described above.

Results and discussion

Oseltamivir was the target selected for exploring the potential of full-system MD studies for the *in silico* screening of candidate MIP systems. A limited scale library of polymer systems was constructed that included five functional monomers reflecting the amino acid-derived functionalities present in the active site of the enzyme neuraminidase (acidic, basic and neutral) (Chart 1).[49,50] Further, three solvents were included in the study: ACN, $CHCl_3$ and MeOH (dielectric constants: 37.5, 4.8 and 32.7, respectively),[51] this group of solvents offers relatively polar (MeOH and ACN) and non-polar ($CHCl_3$), protic (MeOH) and non-protic (ACN and $CHCl_3$) options. The crosslinking monomer used in this study, EGDMA, is soluble in all of the solvents included in this study, as is the initiator AIBN. The elected stoichiometry of polymerization mixture components was based upon experience from the molecular imprinting of templates of similar size as oseltamivir, such as the local anaesthetic bupivacaine[22,52] and the anticoagulant warfarin.[24,53,54]

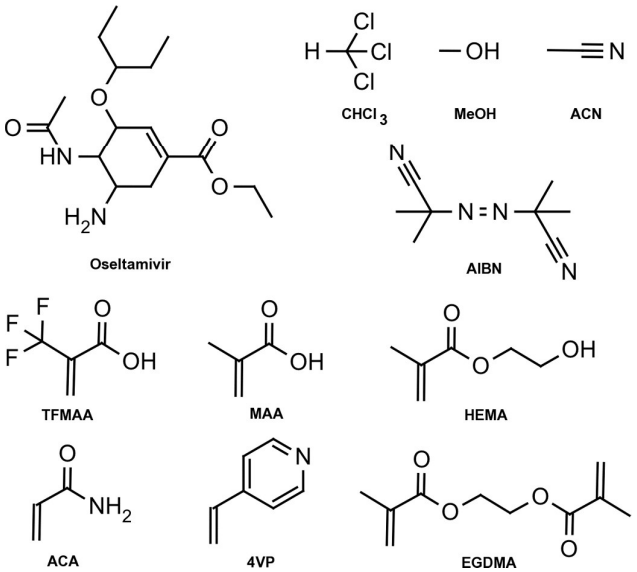

Chart 1 Structures of prepolymerization mixture components. The structures (with atom identifications for atoms studied in hydrogen bond analyses) of prepolymerization mixture components used in the MD studies: the template oseltamivir, the monomers: acrylamide (ACA), 2-hydroxy ethyl methacrylate (HEMA), methacrylic acid (MAA), trifluoromethacrylic acid (TFMAA), 4-vinyl

pyridine (4VP), and ethylene glycol dimethacrylate (EGDMA), the initiator, 2,2'-azobis(isobutyronitrile) (AIBN), and the porogenic solvents chloroform ($CHCl_3$), methanol (MeOH) and acetonitrile (ACN).

Analysis of the extent of hydrogen bonding between the template and the acidic (MAA, TFMAA), neutral (ACA and HEMA) and basic (4VP) functional monomers studied, Figure 1a, revealed significant differences between both the monomers and the influence of solvent (porogen). In non-polar CHCl3, MAA, TFMAA and ACA display the strongest and comparable binding to oseltamivir with 50% of the template molecules engaged in at least one hydrogen bond throughout the simulated 10 ns. HEMA was engaged in lower levels of interaction with the template and 4VP-template interaction was effectively non-existent. Interestingly, although the binding of the neutral functional monomer ACA was found to decrease when switching porogen from CHCl3 to the more polar ACN, average hydrogen bond interactions between oseltamivir and the acidic functional monomers, MAA and TFMAA, were found to increase from approximately 50% engagement in complexation in CHCl3 to complexation throughout nearly the entire 10 ns in the case of ACN. We suggest that the relative differences in behaviour can be explained by the importance of the oseltamivir carbonyl oxygens in the formation of hydrogen bonded functional monomer-template complexes and the relative strengths of the hydrogen bond donating functional groups of the five functional monomers. Here, 4VP was not found to form complexes with the template. The observed decrease in hydrogen bond interaction between ACA and oseltamivir in ACN compared to that observed in CHCl3 suggests that hydrogen bonding between these components predominately involve other chemical functionalities than those involved in MAA/TFMAA-oseltamivir complexation. Changing porogen from the aprotic ACN to MeOH, a protic porogen with a similar polarity, was found to have a profound effect on functional monomer-oseltamivir complexation. In MeOH, the average degree of hydrogen bonding between the functional monomers and oseltamivir was strongly reduced, Figure 1a, due to the highly efficient solvatization of the template by MeOH especially oseltamivir's carbonyl oxygens.

The extent to which the crosslinking monomer EGDMA interacted with the template was considerable, though, interestingly, did not vary significantly between the functional monomers with the exception of 4VP, Figure 1b. However, a clear solvent-dependence of EGDMA-template interaction was observed, with this interaction in CHCl3 being more favorable than in the more polar ACN and MeOH. The greater extent of template-EGDMA interactions in the 4VP polymer was suspected to arise due to the lower degree of competition for interaction of the functional monomer. Although EGDMA in CHCl3 was found to demonstrate an average oseltamivir hydrogen bond complexation to roughly the same extent as that observed for TFMAA, MAA and ACA (50%). The high prevalence of interactions between EGDMA and oseltamivir can be explained by the relatively high abundance of EGDMA relative to functional monomer. Previous analysis of EGDMA-template interactions has suggested that hydrogen bonded complexes involving EGDMA's carbonyl oxygens are associated with shorter lifetimes than the lifetimes of complexes involving the functional monomer, thus giving evidence for the higher affinity of the functional monomer for the template.[21,23,55]

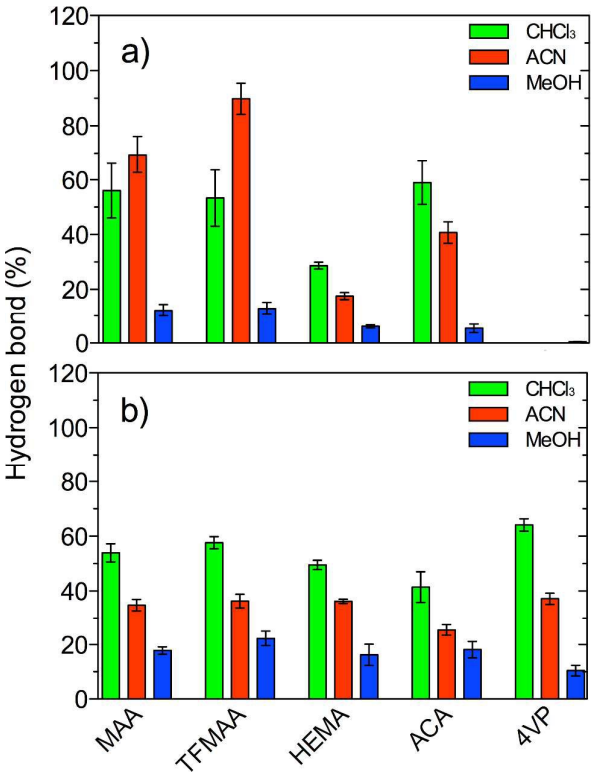

Figure 1 Total average hydrogen bonding (presented as mean ± standard error of the mean, N=4) involving a) the functional monomers, b) the cross-linking monomer, EGDMA, and the template oseltamivir extracted from MD simulations of different solvents ($CHCl_3$, ACN or MeOH) pre-polymerization mixtures.

To gain potential insights concerning the influence of the nature of functional monomer on the final MIP characteristics (*e.g.* surface area, pore size and volume), other hydrogen bonded complexes than those involving the template were examined, Table 2.

Interestingly, the analysis of the degree of functional monomer dimerization revealed, again, the complexity of the interplay between the prepolymerization mixture components, equilibria that ultimately should influence the MIP-oseltamivir recognition behavior. The dimerization of MAA in the $CHCl_3$ solvent system was found to be twice as high as that observed for TFMAA, though these monomers demonstrating a similar degrees of hydrogen bonding to oseltamivir. This is in contrast to an ten-fold difference observed in an NMR-study of a series of ephedrine imprinting systems by Ansell and Wang,[56] who highlighted the impact on polymer performance afforded by TFMAA's oligomerization and potential to form covalent complexes. A change in the porogen from $CHCl_3$ to ACN had only minor influence on self-association. As was discussed for functional monomer-oseltamivir complexation, the introduction of a protic polar porogen, such as MeOH, resulted

in an almost complete disruption of hydrogen bond interactions between the functional monomer and the template. Furthermore, MeOH had the same effect on functional monomer dimerization. Interestingly, of the functional monomers investigated, the greatest degree of dimerization was observed for ACA in the non-polar solvent $CHCl_3$, a behavior that may be explained by the capacity of the amide nitrogen to donate two hydrogen bonds. The relatively high degree of dimerization found for this functional monomer in $CHCl_3$ (17.7%) was much lower in ACN and MeOH thus indicating the relative weakness of the formed ACA-ACA dimers. The dimerization of HEMA while low in comparison to the other functional monomers again followed the trend to stronger hydrogen bonding based interactions in less polar solvents.

Table 2. Average hydrogen bond occupancy[a] per monomer in percentage of the total simulation time (10 ns).

	Porogen Solvation		Dimerization			EGDMA Interaction		
Monomer	ACN	MeOH	$CHCl_3$	ACN	MeOH	$CHCl_3$	ACN	MeOH
MAA	5.0	116.0[b]	10.7	7.7	1.8	61.1	50.7	19.7
TFMAA	4.3	98.6	4.4	3.3	1.2	72.8	61.3	19.0
HEMA	4.6	126.2	2.0	0.7	0.6	29.2	23.2	12.1
ACA	6.6	143.7	17.7	5.1	0.1	37.1	23.5	12.8
4VP[c]		33.5						

[a] The standard error of the mean for presented mean values (N=4) was always ≤ 1.0 % [b] 100% occupancy means that on average one hydrogen bond is formed throughout the simulation, values >100% reflect higher degrees of hydrogen bonding. [c] Not further evaluated due to lack of interactions.

Functional monomer interaction with EGDMA varied both with respect to monomer functionality and solvent. The acidic functional monomers MAA and TFMAA had a higher degree of interaction with EGDMA than the neutral functional monomers, ACA and HEMA, 4VP forming no discernible interactions. Interestingly, the degrees of dimerization observed for the acidic functional monomers MAA and TFMAA appeared to be an inversely proportional with respect to the extent of their interaction with EGDMA. The interplay of template – functional monomer – crosslinker equilibria was recently demonstrated to influence the availability of functional monomer.[57] The frequency and stability of the interaction of EGDMA with MAA and TFMAA reflected the importance of the contribution of the acidic protons of these monomers in the forming interactions, as has been highlighted in modeling and NMR studies by us[57,58] and others.[59–61]

The influence of solvent hydrogen bonding capacity was investigated by comparing ACN and MeOH, solvents that despite similar dielectric constants (ε_{ACN}=37.5 and ε_{MeOH} =32.7),[51] demonstrated large differences in solvation properties. The functional monomers with both hydrogen bond accepting and donating groups had on average one molecule of MeOH bound to each of the 120 molecules of the functional monomer throughout the 10 ns simulation (e.g. MAA ≈ 116% and TFMAA 98.6%, Table 1). These figures dropped to roughly 5% in the case of ACN. The efficiency of MeOH as a solvent effectively competes with the monomers for interaction with the template. Furthermore, the degrees of template dimerization and the extent of hydrogen bonding of template and monomers to the initiator AIBN were examined. In all simulations these events were found to be negligible (<1%).

Polymer synthesis & physical characterization

The oseltamivir imprinted and non-imprinted reference polymers corresponding to those used in the MD studies were synthesized. The monolithic bulk polymers, Syntheses performed in ACN and $CHCl_3$ resulted in polymer monoliths which were ground, sieved through 25 and 63 μm mesh sieves, sedimented repeatedly from acetone and washed extensively as described previously.[52] Polymers synthesized using MeOH as porogen were highly fragile and disintegrated upon light contact to form a fine powder that passed through 10 μm mesh sieves and was difficult to sediment. This indicated that the particles were relatively small, and SEM images (SI, Figures S6-S11) revealed the particles had diameters of around 1 μm. As they could not be used in the subsequent washing steps they were not examined in subsequent binding experiments.

SEM studies were performed on the MIP and REF polymers synthesized in $CHCl_3$ and ACN and even on some REF polymers synthesized in methanol. Polymers synthesized in ACN had a more porous appearance than polymers synthesized in $CHCl_3$ as reflected data from surface area (BET) and porosity (BJH) studies results (SI, Table S2). The SEM images of polymers synthesized in methanol showed aggregates of globular structures. Particle size distributions were determined by laser diffraction and revealed comparable particle size distributions (SI, Figure S12 – S16, Table S3).

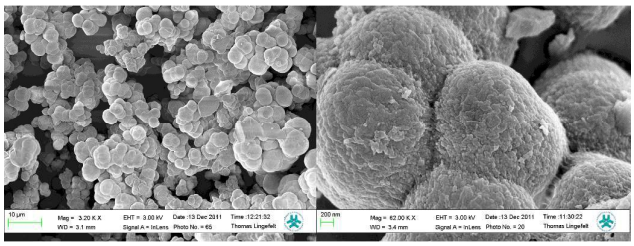

Figure 2 Scanning Electron Microscopy (SEM) images of the REF polymer with HEMA as functional monomer and synthesized in MeOH. The image to the left magnified 3200 x shows the agglomerated globular structures in clusters and the image to the right shows a 62000 x magnification of globular particles. The globular structures to the right are approximately 1.5 μm in diameter.

Elemental analysis and diffuse reflectance FT-IR spectroscopic studies of the MIP and corresponding REF polymers showed no significant differences between the imprinted and corresponding REF polymers, nor were differences observed between polymers prepared in ACN and

$CHCl_3$ (SI, Table S1, Figure S1 – S5). The features of the IR spectra reflected the presence of the anticipated functionalities.

Surface areas (BET) and porosity measurements (BJH) were carried out on each of the polymers in the ACN and $CHCl_3$ series (SI, Table S2). The results from surface area and average pore size studies revealed values for the MAA series that were comparable to previous data.[21,55,58] In general, the variation between systems justifies more detailed studies of the impact of polymer composition on morphology.

Polymer-oseltamivir recognition studies & correlations

The affinities for the template of the ten imprinted and corresponding reference polymers from the $CHCl_3$ and ACN series were investigated by radioligand binding studies. The first studies were polymer titrations performed using a constant amount of [^{3}H]-oseltamivir and varying amounts of polymer, in order to evaluate the binding capacities of the polymers, Figure 3. The polymers synthesized in ACN were initially evaluated in this solvent, though in the case of the polymers synthesized in $CHCl_3$, toluene was used, due to quenching of photons generated during the liquid scintillation counting process by $CHCl_3$. A series of studies using acetic acid (0.5%, v/v) as a polar modifier acetic acid intended for blocking non-specific sites.

A general trend was that the polymers that had been shown by the MD studies to have the greatest extent of interaction between the template and monomers (functional and EGDMA) demonstrated the greatest affinity for the template, Figure 1 and Figure 3. This was most prominent in the case of the MAA and TFMAA polymers, which the rdf-analyses indicate is due to binding to the carbonyl oxygens of oseltamivir being a frequent and long-lived event. The 4VP polymers, with effectively no functional monomer – template interaction observed in the MD studies of their prepolymerization mixtures, afforded low levels of affinity. HEMA and ACA showed intermediate affinities. It is noteworthy that binding to the ACA polymers was significantly attenuated by the presence of AcOH, which reflects the importance for recognition of the carboxylic acid functionalities of MAA and TFMAA.

A comparison of the differences in binding to non-imprinted and imprinted polymers, which we define as the selective binding, demonstrated significant differences in the cases of MAA and ACA, though notably less so for TFMAA, and no effective differences for HEMA and 4VP. Aside from the case of TFMAA, which while demonstrating strong binding was not notably selective, the observed selectivities again followed the MD-data with respect to the extents of interaction between functional monomers and template in the respective solvents. Of particular interest were the MAA polymers prepared in ACN, where a most prominent difference was observed. As nonpolar media generally facilitate electrostatic interactions contributing to MIP-template recognition, the unprecedented selectivity in the case of the MAA polymer prepared in ACN was a surprise, but had been implied by the MD studies, and appears to arise due to the lower extent of dimerization and interaction with crosslinker that leaves more MAA available for interaction with template (Figure 1 and Table 2). That the MD-studies had identified polymers prepared in ACN with MAA or TFMAA as those with the highest degree of template complexation and that these had the highest affinities and selectivities was not intuitive, and underscored the potential of all-component MD-studies of MIP prepolymerization mixtures for predicting polymer performance. The relative lack of selectivity in the TFMAA systems suggested that strong non-specific interactions were present, perhaps reflecting the presence of significant numbers of ionized TFMAA residues in the polymers, relative to the case of MAA (pK_a 2.1 and 4.7, respectively), when binding in more polar media.[62] A deeper investigation of this is the subject of ongoing work, and even the potential impact of rebinding medium-induced swelling on recognition properties.

The presence of the acidic modifier acetic acid, AcOH, induced a general reduction in overall binding through competition for polar functionalities of the ligand and polymer. However, the influence of AcOH on MIP and REF was not uniform, as was most evident in the case of the MAA polymers, where there was a very notable reduction in the case of the MAA-REF polymers, in particular for that prepared in ACN. This can be interpreted as reflecting fundamental differences in the nano-level structures of the MIP and its corresponding non-imprinted polymer. As this MAA is less engaged in dimerization than TFMAA (as judged by the corresponding MIP prepolymerization mixtures, Table 2) this would afford a greater proportion of "free" (non-associated) monomer species. The impact of AcOH could therefore be attributed to a greater prevalence of free monomer in the MAA polymers, which would contribute to non-specific binding that can be readily pacified by the acidic modifier.

Furthermore, the MIP-oseltamivir rebinding behavior observed for the ACA-MIP prepared in either $CHCl_3$ in which the dimerization of ACA was predicted to be the highest among the systems examined (≈17 %, Table 2) also highlights the fact that other interactions, in particular the contribution of interactions with the crosslinker, must be accounted for in order to make predictions on final polymer rebinding capacity and selectivity. Finally polymers prepared with the functional monomers HEMA and 4VP demonstrated lower oseltamivir binding capacities than the other systems, with effectively no selective binding sites in the MIPs in both non-polar and even polar conditions, in agreement with the results of the all-component MD simulations (see SI, Figure S17 for results from competitive binding studies) The potential impact of the surface areas of the polymers on binding was also examined (SI, Table S2), though in this case did not influence the rank order nor relative differences between the systems studied. The origin of the differences in the morphologies of the polymer systems is of interest and is the subject of ongoing studies in our laboratory.

A series of competitive studies was then undertaken, where displacement of radioligand from each of the MAA-based polymers by cold ligand (SI, Figure S17) was examined in TOL, ACN containing 0.5% AcOH (v/v) or buffer (pH 7.0, 10 mM

phosphate). The amount of polymer used (0.75 mg) was based upon the results of the polymer titration studies. The observed selectivities (MIP vs REF) of the polymers synthesized in ACN and $CHCl_3$ reflected those observed in the earlier polymer titration studies. Interestingly, the polymers prepared in ACN and $CHCl_3$ preformed similarly when the polymers were evaluated in the organic rebinding media (ACN and TOL, both with 0.5% AcOH (v/v)). A move to aqueous buffer saw a general reduction in the affinity of all systems, though selectivity (MIP vs REF) was observed for the polymer synthesized in ACN. Further studies for optimization of binding (pH, ionic strength, organic modifiers, *etc.*) is expected to lead to the identification of conditions for enhanced polymer-ligand affinity and selectivity.

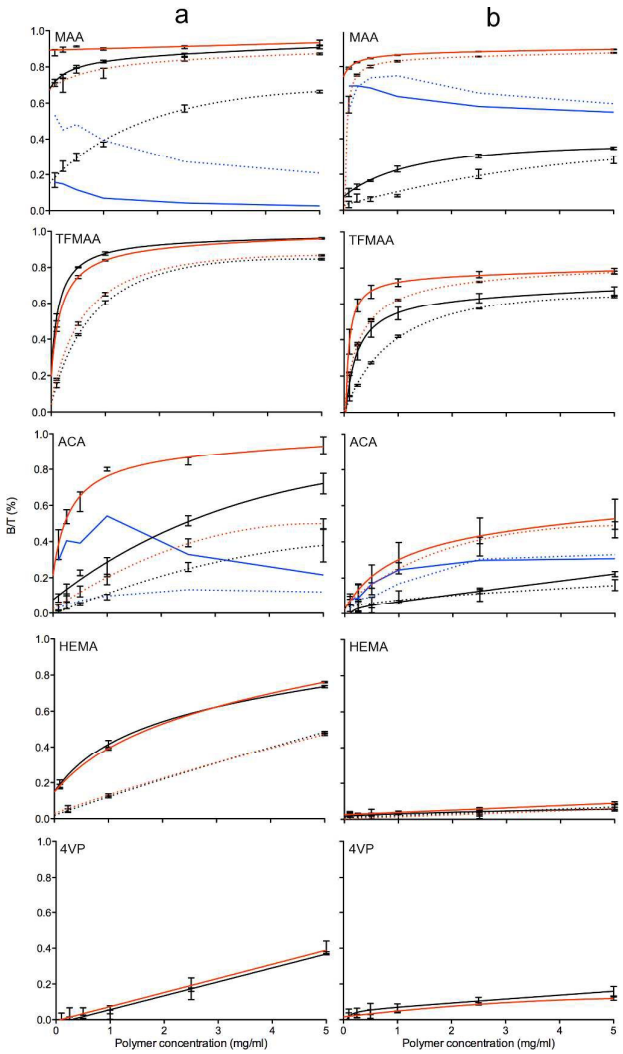

Figure 3 Results from radioligand-polymer titration studies, showing the binding of a constant amount of [^{3}H]-oseltamivir (0.5 pmol) to various concentrations of MIPs (red lines) or REFs (black lines), prepared using different functional monomers in a) $CHCl_3$ or b) ACN. Studies including AcOH (0.5 %, v/v, dashed lines). For selected systems, the specific binding, here defined as the difference in binding to MIP and REF polymers, is shown as blue lines.

Conclusions

We have deployed a series of all-component (full-system) MD-based studies to probe a library of candidate oseltamivir molecularly imprinted polymer prepolymerization mixtures. The polymers included one of five functional monomers (ACA, HEMA, MAA, TFMAA, 4VP) and three solvents (ACN, $CHCl_3$, MeOH). Analysis of the respective prepolymerization mixtures revealed considerable differences in the nature of the ensembles of interactions between the template and the functional and crosslinking monomers. Polymer-template affinity studies were performed using radioligand binding assays in a range of media and the results demonstrated good correlations between the extent of complexation of the template by the functional monomers in the simulated prepolymerization mixtures and the affinity of the subsequent polymer for the template. A further feature of this study was an insight into the impact of solvent on polymer morphology, in particular the connection between the high degree of solvatization of polymerization mixture components by methanol observed in the MD studies and the fragile, nanoparticle nature of the corresponding polymers. The influence of polymer morphology on recognition has been highlighted in recent studies with MAA-EGDMA-based polymers.[55] Competitive binding studies demonstrated that the MAA-based MIP prepared in ACN maintained selectivity in aqueous buffer. Efforts are now underway to investigate the application of some of the polymers derived from this study as matrices for the solid phase extraction of oseltamivir and as potential catalysts for glycosidic bond hydrolysis and formation. Collectively, these studies have demonstrated the potential for using all-component molecular dynamics studies as a prognostic tool for the rational design of molecularly imprinted polymers. Importantly, this study highlights the complexity of the prepolymerization mixture and the importance of holistic treatments in the development of tools for the prediction of polymer molecularly imprinted polymer performance. To focus solely on functional monomer-template interactions can be misleading, as reflected in the clear contributions of solvent and crosslinking monomers to template complexation.

Acknowledgements

The authors thank Dr. Håkan S. Andersson and Dr. Annika M. Rosengren, both Linnaeus University, for valuable discussions. The financial support of Linnaeus University and the Swedish Research Council (2006-6041 and 2014-4573) are acknowledged. The simulations were performed on resources provided by the Swedish National Infrastructure for Computing (SNIC) at LUNARC (SNIC-001/12-141 and 2013/1-192).

References

1 W. G. Wood, *Clin. Lab.*, 2008, **54**, 423–438.
2 I. Y. Galaev and B. Mattiasson, *Trends Biotechnol.*, 1999, **17**, 335–340.

3 C. Alexander, H. S. Andersson, L. I. Andersson, R. J. Ansell, N. Kirsch, I. A. Nicholls, J. O'Mahony and M. J. Whitcombe, *J. Mol. Recognit.*, 2006, **19**, 106–180.
4 G. Wulff, *Chem. Rev.*, 2002, **102**, 1–28.
5 K. Haupt and K. Mosbach, *Chem. Rev.*, 2000, **100**, 2495–2504.
6 T. Takeuchi, D. Fukuma and J. Matsui, *Anal. Chem.*, 1999, **71**, 285–290.
7 K. J. Shea and E. Thompson, *J. Org. Chem.*, 1978, **43**, 4253–4255.
8 M. J. Whitcombe, N. Kirsch and I. A. Nicholls, *J. Mol. Recognit.*, 2014, **27**, 297–401.
9 M. J. Whitcombe, I. Chianella, L. Larcombe, S. A. Piletsky, J. Noble, R. Porter and A. Horgan, *Chem. Soc. Rev.*, 2011, **40**, 1547–1571.
10 C. J. Allender, C. Richardson, B. Woodhouse, C. M. Heard and K. R. Brain, *Int. J. Pharm.*, 2000, **195**, 39–43.
11 B. Sellergren, *Molecularly Imprinted Polymers: Man-Made Mimics of Antibodies and their Application in Analytical Chemistry*, Elsevier, Amsterdam, 2001, vol. 23.
12 G. Vlatakis, L. I. Andersson, R. Müller and K. Mosbach, *Nature*, 1993, **361**, 645–647.
13 C. J. Allender, K. R. Brain and C. M. Heard, *Prog. Med. Chem.*, 1999, **36**.
14 J. Svenson and I. A. Nicholls, *Analytica Chimica Acta*, 2001, **435**, 19–24.
15 J. O'Mahony, B. C. G. Karlsson, B. Mizaikoff and I. A. Nicholls, *Analyst*, 2007, **132**, 1161–1168.
16 F. Lanza and B. Sellergren, *Chromatographia*, 2001, **53**, 599–611.
17 A. M. Rosengren, J. G. Karlsson, P. O. Andersson and I. A. Nicholls, *Anal. Chem.*, 2005, **77**, 5700–5705.
18 I. A. Nicholls, H. S. Andersson, K. Golker, H. Henschel, B. C. G. Karlsson, G. D. Olsson, A. M. Rosengren, S. Shoravi, S. Suriyanarayanan, J. G. Wiklander and S. Wikman, *Anal. Bioanal. Chem.*, 2011, **400**, 1771–1786.
19 I. A. Nicholls, H. S. Andersson, C. Charlton, H. Henschel, B. C. G. Karlsson, J. G. Karlsson, J. O'Mahony, A. M. Rosengren, J. K. Rosengren and S. Wikman, *Biosens. Bioelectron.*, 2009, **25**, 543–552.
20 I. A. Nicholls, B. C. G. Karlsson, G. D. Olsson and A. M. Rosengren, *Ind. Eng. Chem. Res.*, 2013, **52**, 13900–13909.
21 B. C. G. Karlsson, J. O'Mahony, J. G. Karlsson, H. Bengtsson, L. A. Eriksson and I. A. Nicholls, *J. Am. Chem. Soc.*, 2009, **131**, 13297–13304.
22 J. G. Karlsson, B. Karlsson, L. I. Andersson and I. A. Nicholls, *Analyst*, 2004, **129**, 456–462.
23 G. D. Olsson, B. C. G. Karlsson, S. Shoravi, J. G. Wiklander and I. A. Nicholls, *J. Mol. Recognit.*, 2012, **25**, 69–73.
24 B. C. G. Karlsson, A. M. Rosengren, I. Näslund, P. O. Andersson and I. A. Nicholls, *J. Med. Chem.*, 2010, **53**, 7932–7937.
25 G. D. Olsson, B. C. G. Karlsson, E. Schillinger, B. Sellergren and I. A. Nicholls, *Ind. Eng. Chem. Res.*, 2013, **52**, 13965–13970.
26 E. Schillinger, M. Möder, G. D. Olsson, I. A. Nicholls and B. Sellergren, *Chem-Eur. J.*, 2012, **18**, 14773–14783.
27 D. Cleland, G. D. Olsson, B. C. G. Karlsson, I. A. Nicholls and A. McCluskey, *Org. Biomol. Chem.*, 2014, **12**, 844–853.
28 J. O'Mahony, M. Moloney, M. McCormack, I. A. Nicholls, B. Mizaikoff and M. Danaher, *J. Chromatogr. B.*, 2013, **931**, 164–169.
29 Y. Yang, J. Li, Y. Liu, J. Zhang, B. Li and X. Cai, *Anal Bioanal Chem*, 2011, **400**, 3665–3674.
30 E. De Clercq, *Nat. Rev. Drug Discov.*, 2006, **5**, 1015–1025.
31 A. Moscona, *N. Engl. J. Med.*, 2005, **353**, 1363–1373.
32 L. V. Gubareva, L. Kaiser and F. G. Hayden, *Lancet*, 2000, **355**, 827–835.
33 M. von Itzstein, *Nat. Rev. Drug Discov.*, 2007, **6**, 967–974.
34 M. D. de Jong, T. T. Thanh, T. H. Khanh, V. M. Hien, G. J. D. Smith, N. V. Chau, B. V. Cam, P. T. Qui, D. Q. Ha, Y. Guan, J. S. M. Peiris, T. T. Hien and J. Farrar, *N. Engl. J. Med.*, 2005, **353**, 2667–2672.
35 A. Moscona, *N. Engl. J. Med.*, 2005, **353**, 2633–2636.
36 Q. M. Le, M. Kiso, K. Someya, Y. T. Sakai, T. H. Nguyen, K. H. L. Nguyen, N. D. Pham, H. H. Ngyen, S. Yamada, Y. Muramoto, T. Horimoto, A. Takada, H. Goto, T. Suzuki, Y. Suzuki and Y. Kawaoka, *Nature*, 2005, **437**, 1108–1108.
37 A. Gillman, S. Muradrasoli, H. Söderström, J. Nordh, C. Bröjer, R. H. Lindberg, N. Latorre-Margalef, J. Waldenström, B. Olsen and J. D. Järhult, *PLoS ONE*, 2013, **8**, e71230.
38 D. A. Case, T. A. Darden, T. E. (III) Cheatham, C. L. Simmerling, J. Wang, R. E. Duke, R. Luo, M. Crowley, R. C. Walker, W. Zhang, K. M. Merz, B. Wang, S. Hayik, A. Roitberg, G. Seabra, I. Kolossváry, K. F. Wong, F. Paesani, J. Vanicek, X. Wu, S. R. Brozell, T. Steinbrecher, H. Gohlke, L. Yang, C. Tan, J. Mongan, V. Hornak, G. Cui, D. H. Mathews, M. G. Seetin, C. Sagui, V. Babin and P. A. Kollman, *Amber 10*, University of California, San Francisco, 2008.
39 D. A. Pearlman, D. A. Case, J. W. Caldwell, W. S. Ross, T. E. (III) Cheatham, S. DeBolt, D. Ferguson, G. Seibel and P. Kollman, *Comput. Phys. Commun.*, 1995, **91**, 1–41.
40 D. A. Case, T. E. (III) Cheatham, T. Darden, H. Gohlke, R. Luo, K. M. Merz, A. Onufriev, C. Simmerling, B. Wang and R. J. Woods, *J. Comput. Chem.*, 2005, **26**, 1668–1688.
41 L. Martínez, R. Andrade, E. G. Birgin and J. M. Martínez, *J. Comput. Chem.*, 2009, **30**, 2157–2164.
42 J. M. Martínez and L. Martínez, *J. Comput. Chem.*, 2003, **24**, 819–825.
43 J. Wang, P. Cieplak and P. A. Kollman, *J. Comput. Chem.*, 2000, **21**, 1049–1074.
44 J. Wang, R. M. Wolf, J. W. Caldwell, P. A. Kollman and D. A. Case, *J. Comput. Chem.*, 2004, **25**, 1157–1174.
45 T. E. (III) Cheatham, J. L. Miller, T. Fox, T. A. Darden and P. A. Kollman, *J. Am. Chem. Soc.*, 1995, **117**, 4193–4194.
46 Y. Hayashi, H. Ishikawa, Process for Producing Oseltamivir Phosphate and Intermediate Compound. WO2009145263 (A1), December 3, 2009.
47 S. Brunauer, P. H. Emmett and E. Teller, *J. Am. Chem. Soc.*, 1938, **60**, 309–319.
48 E. Barrett, L. Joyner and P. Halenda, *J. Am. Chem. Soc.*, 1951, **73**, 373–380.
49 P. M. Colman, *Protein Sci.*, 1994, **3**, 1687–1696.
50 M. Vonitzstein, W. Wu, G. Kok, M. Pegg, J. Dyason, B. Jin, T. Phan, M. Smythe, H. White, S. Oliver, P. Colman, J. Varghese, D. Ryan, J. Woods, R. Bethell, V. Hotham, J. Cameron and C. Penn, *Nature*, 1993, **363**, 418–423.
51 D. R. Lide, *CRC Handbook of Chemistry and Physics*, CRC Press, Boca Raton, FL., 81st Ed.
52 J. G. Karlsson, L. I. Andersson and I. A. Nicholls, *Analytica Chimica Acta*, 2001, **435**, 57–64.
53 A. M. Rosengren, B. C. G. Karlsson, I. Näslund, P. O. Andersson and I. A. Nicholls, *Biochemical and Biophysical Research Communications*, 2011, **407**, 60–62.
54 A. M. Rosengren, B. C. G. Karlsson and I. A. Nicholls, *International Journal of Molecular Sciences*, 2013, **14**, 1207–1217.
55 K. Golker, B. C. G. Karlsson, G. D. Olsson, A. M. Rosengren and I. A. Nicholls, *Macromolecules*, 2013, **46**, 1408–1414.
56 R. J. Ansell and D. Wang, *Analyst*, 2009, **134**, 564–576.
57 S. Shoravi, G. D. Olsson, B. C. G. Karlsson and I. A. Nicholls, *International Journal of Molecular Sciences*, 2014, **15**, 10622–10634.
58 J. Svenson, J. G. Karlsson and I. A. Nicholls, *J. Chromatogr. A*, 2004, **1024**, 39–44.

59 B. Sellergren, M. Lepistö and K. Mosbach, *J. Am. Chem. Soc.*, 1988, **110**, 5853–5860.
60 M. J. Whitcombe, L. Martin and E. N. Vulfson, *Chromatographia*, 1998, **47**, 457–464.
61 R. J. Ansell and K. L. Kuah, *Analyst*, 2005, **130**, 179–187.
62 H.-F. Wang, Y.-Z. Zhu, J.-P. Lin and X.-P. Yan, *Electrophoresis.*, 2008, **29**, 952–959.